International Journal of GEOMATE, July 2023, Vol. 25, Issue 107, pp.173-182
ISSN: 2186-2982 (P), 2186-2990 (O), Japan, DOI: https://doi.org/10.21660/2023.107.g12203
Geotechnique, Construction Materials and Environment

DECREASING THE QUALITY OF WATER RESOURCES IN THE RAWAS WATERSHED DUE TO LAND DEGRADATION

Zainuddin Muchtar[1], Febrian Hadinata[2*], Dinar Dwi Anugerah Putranto[3]

[1]Doctoral Program in Engineering, Postgraduate Program, Faculty of Engineering, Universitas Sriwijaya;
[2,3] Department of Civil Engineering and Planning, Faculty of Engineering, Universitas Sriwijaya, Indonesia

*Corresponding Author, Received: 28 March 2022; Revised: 24 March. 2023; Accepted: 02 April 2023

ABSTRACT: There is an urgent need to regulate and monitor land degradation through quantitative assessments and mapping critical land to increase national capacity as stated in the Sustainable Development Goals (SDGs). This can be achieved by introducing an innovative approach to monitoring the necessary land at the national, provincial, and district city levels. Moreover, the sub-watershed scale analysis associated with the distribution of degraded land through multi-temporal geospatial layers [1,2] helps provide a regionally consistent dataset needed to support the agendas aligned with sustainable development goals (SDGs) [3]. The analysis of topographical conditions, types of land cover, and the amount of kinetic energy for rain intensity of 30 minutes with a return period of 2 to 100 years is the basis for predicting critical land using the RUSLE method [4]. Predicted essential distribution of land and potential for land degradation that occurred in the last 10 years (2010-2020), covering an area of 2,215,303 Km^2 (37.95%) land in the critical category, 10,780 Km^2 (0.18%) very critical, 629,301 Km^2 (10.78%) is slightly critical, 2,256.92 Km^2 (38.7 %) potentially critical and only 725,875 Km^2 (12.43%) which is not vital. The most dominant problem of watershed degradation is land cover loss due to forest encroachment in areas with slopes over 25%. The expansion of land conversion is typical of oil palm plantations, which triggers soil erosion, flooding, and a decrease in pristine water quality due to river water pollution.

Keywords: Critical land, Kinetic energy, Land cover, Land degradation.

1. INTRODUCTION

The pressure on land resources, coupled with the intensive rainfall linked to climate change, is causing land degradation. Furthermore, it has been reported that excessive rainfall and human activities such as logging and inappropriate land development are increasing the occurrence of run-off and soil erosion [5]. Therefore, it is essential to monitor the changes in the periodic degradation of land in order to preserve environmental quality as well as improve natural resource management and land planning [6].

Several cases of land degradation have caused the deterioration of pristine water quality. This is due to high soil erosion, which causes increased sedimentation that enters rivers and pollutes raw water sources from surface water [7]. Increased soil erosion, caused by inappropriate land management, can be used as a parameter in monitoring land degradation. However, the technique of monitoring land degradation by calculating the amount of erosion by analyzing the ratio of land use change on various classifications of different slopes, coupled with the analysis of the amount of rainfall that occurs in the watershed area, is a better parameter in monitoring land degradation [8,9]. From several studies, some argue that in a healthy forest area, soil erosion will be hampered by the lower vegetation and the existing lining of the litter [10]. The smaller the litter layer, the more soil erosion content will occur. Ecological pressure can also be caused by a regional development that suppresses the upstream watershed area [11]. Pollution and sedimentation can also happen because they pay less attention to good land management in the upstream watershed area.

The Rawas watershed is one part of the sub-watershed in the Musi River Basin, which has experienced a decrease in the quality of clean water. Based on water quality measurement data at several points along the flow of the Rawas, Rupit, and Kuis rivers, from 2019-2021, the quality of Total dissolved solids (TDS) is increasingly worrying (see Figure 1). From these data, it can be concluded that the raw river water quality is decreasing due to high pollution caused by the illegal mining of gold ore and iron ore in the upstream watershed area.

The data retrieved from the Musi Watershed Management Center (BPDAS MUSI) in 2019 [12] showed that critical land categorized as very essential in the Rawas watershed area is 5,838.183 $Km^{2,}$ while those classified as moderately necessary is 2,215.303 Km^2, the required potential is 2,256.94 Km^2, and the non-critical is 725.825 Km^2.

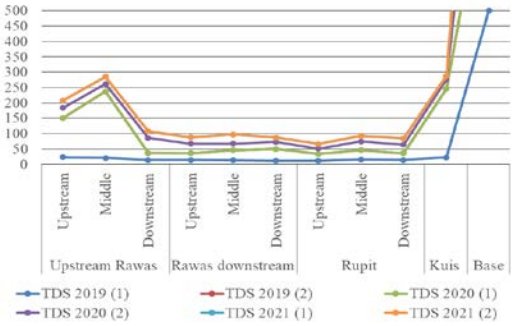

Fig. 1. TDS value at river of rawas watershed

2. RESEARCH SIGNIFICANCE

The optimization of land usage is one of the critical activities required to ensure the appropriate distribution of land. It can be achieved by modeling the topographic conditions, types of land cover, duration and time of rain, and the magnitude and distribution of erosivity using GIS techniques. This is necessary to provide the data needed to predict the critical land distribution and potential environmental damage in the watershed area.

The critical land analysis method discussed in this study focuses on combining land use change data and different additional datasets through a more flexible essential land estimation technique. Moreover, the sub-watershed scale related to the distribution of necessary land was analyzed using multi-temporal geospatial layers [11]. This method assists in providing a regionally consistent set of critical land distribution data to support the agendas of sustainable development goals (SDGs), specifically SDG indicator 15.3.1 focused on the proportion of degraded land over the total land area [13].

3. METHODOLOGY

3.1 Study Area

The Rawas sub-watershed is one of the 36 water facilities in the south Sumatra province administrative region and is also part of the Musi river basin. The facility has a catchment area (DAS) with a geographical location at variational coordinates of 102° 4' 4.8" – 103° 27' 36" east longitude and 2° 19' 15" – 3° 06' 36" south latitude. The upstream area is at an altitude of 2,100 m above sea level and it is one of the highest peaks in the Kerinci Seblat national park zone which is partly included in the administrative region of north Musi Rawas regency (1,884.61 Km2 or 32%). Moreover, Kerinci Seblat National Park (TNKS) is part of the global warp designated by UNESCO as a world heritage area with more than 4000 species of primary forest flora and 115 species of ethnobotanical plants. There are two significant rivers or sub-river systems flow in the Rawas sub-watershed and these include the Rupit river which fulfills and empties into the rawas water body.

The water resources in the sub-systems of Rawas and Rupit rivers have benefited the residents in the watersheds. However, the licensing development for several lands utilized for plantation activities is increasing massively in the area. This indicates an imbalance in water availability during the rainy and dry seasons, as observed in other river systems within the Musi river basin [14,15]. It was also discovered that the provincial and district governments issued several permits for oil palm and rubber plantations, mining, infrastructure, and other economic developments, as well as many illegal operations in the hills and along rawas river to extract coal, gold, sand, and Iron ore. These activities are disrupting the raw water supply system and causing an increase in erosion magnitude and flooding volume.

3.2 Methods

The rainfall-run-off was modeled using the RUSLE analysis technique [16]. This involved the utilization of GIS to assess the criticality level of land based on the relationship between soil properties, slope diversity, land use patterns, and the amount of erosion. Moreover, the physical parameters of the watershed were combined with time series of high rainfall in the watershed area. This was achieved by calculating the amount of kinetic energy (annual Kinetic Energy) caused by the rain intensity (precipitation) within 30 minutes for several return times variations. The RUSLE model was used to analyze all parameters in the watershed to estimate the magnitude of detachment indexes or the amount of surface soil detachment with the potential to become a sediment solution, depending on the slope level, soil structure, and land use [17].

The land use data were used to redistribute the aggregate number of critical lands in order to increase the accuracy of the distribution data based on regional scale sizes [18]. Moreover, several factors associated with environmental damage correlate with the methods applied by humans in distributing land for different activities in the landscape [19]. This means it is possible to use a large number of land use groups to effectively model the different distribution areas of critical land within the watershed boundary unit and to better describe the degraded land [20].

3.2.1 Extraction of Land Use

Multispectral image classification was applied as the basis for multitemporal monitoring of land use and landform maps generated through the digital interpretation of images [21]. For example, the relationship between an area with low-level

vegetation land cover and plain fluvial landforms is a characteristic of paddy land. The other elements of interpretation such as patterns, shapes, sizes, and associations were also considered in identifying land use objects. This was achieved digitally by recognizing objects and processing spectral values. Previous works found that when forests are converted to artificial forests [22], soil is reduced.

3.2.2 Extraction of Drainage Network

Digital Elevation Model (DEM) is the digital data with x, y, and z values. The x and y values are the coordinates of the position or location while the z values are used for the elevation. This model can be derived or used to generate new data that requires altitude information such as contour maps, elevation maps, land slope class maps, digital terrain models (DTM), hill shading, aspect maps, intervisibility (visible), slope length, watershed shape, watershed density, and others [23].

The DEM data used in this study is DEM Nas (Digital Elevation Model National Indonesia) in the form of raster data with pixel values of 7,5 m indicating the location coordinates and altitude values.

Morphological parameters are very important to watershed features and proper watershed management planning[24][25]. It has also been reported that geological, geomorphological, land cover, and hydrological information are beneficial to understanding watershed drainage patterns. The presentation of watershed morphometric conditions is expected to provide a comprehensive picture of the drainage basin and this is very useful in watershed environmental management, hydrological modeling, conservation, and restoration [26].

3.2.3 Soil Loss Modeling

The soil loss determination method has two different base phases. The first is the water phase with the kinetic energy of rainfall, overland flow, and annual precipitation values. The second is the sedimentation phase with the rate of soil detachment due to the impact of raindrops and the calculation of transport capacity of overland flow values for every pixel by generating maps for each input data [27]. Moreover, the predictive model applied to assess soil erosion risk is called the Morgan model with the input parameters and operating functions listed as follows. It is important to note that the strength of the energy generated from the volume of rainfall is half the mass of the particle times the square area of the soil surface. Furthermore, the amount of erosion was calculated using EI_{30} developed by Wischmeter and Smith, 1978 [28].

The sediment transport flow was modeled by estimating mass conservation to simulate soil erosion and deposition. The average change in soil loss was also predicted through the following RUSLE equation [29],

$$\boldsymbol{E = R.K.LS.C.P} \quad (1)$$

where E is the computed soil erosion rate (annual average) (tons/ha/year), R is the rain erosivity index (MJ mm/ha/h/year), K is the soil erodibility index (tons.ha.h/MJ/mm), LS is the index of slope length and slope steepness factor, C is the vegetation cover index, and P is the index of tillage or soil conservation measures.

The amount of rainfall (R) in g/m^2, is a function of an increase in the kinetic energy, and has a strong correlation with soil loss. It defined as product of the maximum intensity of rainfall over a 30 minutes [27]

$$R = \frac{1}{n}\sum_{j=1}^{n}\sum_{k=1}^{mj}(\boldsymbol{E}\, I_{30})\boldsymbol{k} \quad (2)$$

where n is the number of years included in the analysis, *mj* is the number of erosive events during year *j*, and EI_{30} (MJ mm/ha/h) is the R for event k.

For a particular event, erosivity is calculated as follows [27]:

$$E\,I_{30} = (\sum_{r=1}^{m} er.vr).\, I_{30} \quad (3)$$

where er is the kinetic energy per unit of rainfall (MJ/ha/mm); vr is the rainfall depth (mm) for the hydrograph's time interval r; r is subdivide into m sub-intervals; I_{30} is the maximum rainfall intensity for a 30-minute timeframe

The *LS* factor was calculated to predict the strength/erosivity of the run-off and was expressed as the ratio of slope steepness affected soil loss and β is slope gradient in degree. By classifying the slope of the watershed according to y values shown in Table 1 that vary from 0.2 in the upper part of the watershed to 0.5 in the downstream and middle of the watershed was generated to run Eq. (4).

$$LS = (\frac{QaM}{22.13})^{y}(65.4\, Sin^2\beta + 4.56\, Sin\beta + 0.0654) \quad (4)$$

Qa is flow accumulation and M is cell size (Wischmeter and Smith, 1978) [30],

Table 1 **y** values for a range of slope classes

Slope class (%)	y value
< 1	0.2
1 - 3	0.3
3 - 5	0.4
>5	0.5

3.2.4. Transport Sediment

The model's sediment transport capacity (T) is a function of the overland flow volume and slope (S) coverage factor. The overland flow (Q) is the derivative of the annual rainfall (R), the ratio between soil moisture storage, and the separation of yearly rainfall with the number of daily rains per year (n) [31]. Meanwhile, the soil moisture storage (Rc) was based on the field capacity (Ms), bulk density (Bd), root depth and topsoil, and the ratio of actual evapotranspiration (EPT). It is also important to note that the plant factor (c) was obtained from the land cover sub-factor, therefore, the equation becomes [21]

where S is Slope (radians), and C is land cover factor

$$\boldsymbol{Q = R * e^{\frac{Rc}{Ro}}} \text{ mm} \quad (6)$$

where R is average annual precipitation (mm)

$$Rc = 1000 * Rd * Ms * Bd * (Ea/Ep)^{0,5} \quad (7)$$

where Rd is the depth of root zone (m), Ms is soil moisture at field capacity (w/w), Bd is bulk density on Top Soil (g/Cm2), Ea/Ep is ratio of actual and potential evapotranspiration, Ro = R/n, n is number of rainy days in a year.

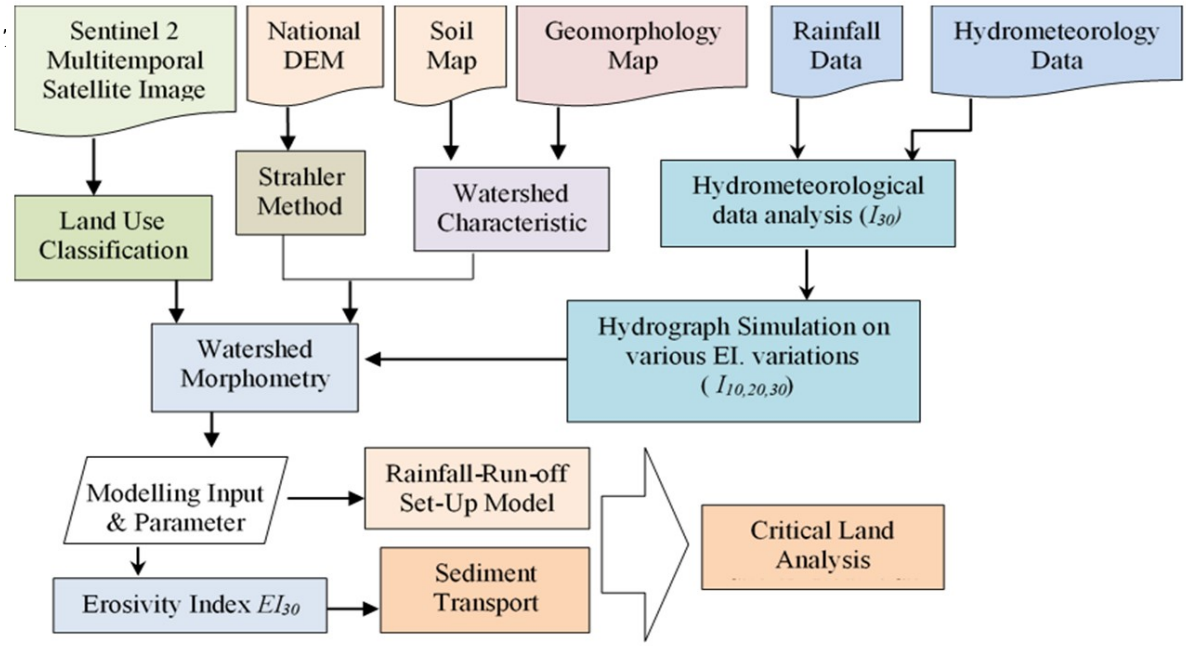

Fig. 2 Research flowchart

4. RESULT AND DISCUSSION

4.1 Watershed Morphometric Analysis

The morphometric analysis was based on the data obtained on the elevation of the watershed area, the aspect of the site, as well as the gradient and slope of the land contributing to the drainage basin. The analysis was used to understand the hydrogeological behavior of drainage basins and to determine the climatic, geological, geomorphological, and structural conditions of the area.

The analysis of the drainage in the watershed system was used to determine the status of the flow pattern, inundation area, and availability of water in the study area (see Table 2).

4.1.1 Flow Length

Flow length is one of the essential hydrological characteristics in a watershed area due to its ability to provide information on run-off characteristics. The size of the most extended river flow in the Rawas sub-watershed is 94.42 Km with slope drain is 3.38 %, while the shortest length is 54,66 Km with slope drain is 0.13 % (see Table 2). All the drainage channels in the sub-system were observed to be elongated patterns without many river branches. Therefore, it was concluded that the Rawas sub-watershed is a basin with alluvial deposits of former sediment or river overflow.

4.1.2. Average Flow Length (L)

Average flow length is a dimensionless property that expresses the characteristic size of the drainage network and watershed surface components contributing to the arrival time of water flow from upstream to downstream. For example, the average flow length in the Rawas watershed is 73.33 Km.

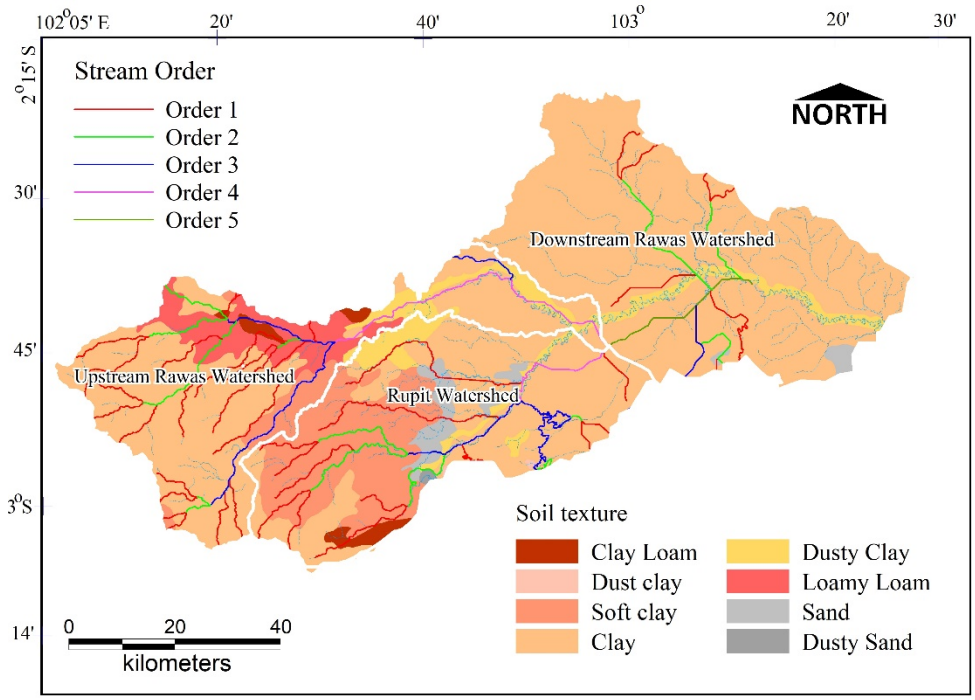

Fig. 3 Watershed morphometry and soil texture

Table 2 Morphometric of rawas river watershed

No.	Name of watershed	Watershed area (Km2)	Stream length (Km)	Perimeter (P) Km	Drainage density (Km/Km2)	Slope drain (%)
1	Uper rawas watershed	1,782.94	94,42	339.8	0.397	3.38
2	Downstream rawas watershed	2,280.92	54.66	272.1	0.359	0.13
3	Rupit watershed	1,824.17	71.04	260.8	0.288	1.51

4.1.3. Basin Area (A)

The watershed area is another crucial paramter like the length of river drainage. It was discovered that the downstream rawas watershed has the largest catchment area with 2,280.92 Km2 and the smallest size is 1,782.940.75 Km2.

4.1.4. Basin Perimeter (P)

The basin's perimeter is the outermost boundary of the watershed which is commonly known as the circumference of the sub-watershed .It was measured along the border between adjacent watersheds and used as an indicator of its size and shape. The perimeter of the basin of the study area varies and the largest circumference was recorded to be 339.8 Km.

4.1.5. Drainage Pattern

The drainage pattern in the basin reflects the influence of slope, lithology, and rock structure. Its analysis usually assists in identifying the stages of the erosion cycle. It also presents several characteristics of the watershed through the pattern and texture of the drainage. The Rawas watershed was observed to have an elongated drainage pattern and trails and this means the study area is flat and undulating with one extensive river system and a floodplain basin.

4.1.6. Drainage Density

Drainage density is the flow length per unit area of a basin or watershed and serves as another element of drainage analysis. It was discovered that the drainage density of the Rawas basin is 0.397 Km/Km2.

4.2. Topography

The research area is one of the upper reaches of the Musi river basin with an altitude of 2,100 m above sea level and the lowest area at an altitude of 25 m above sea level. The slope of the Rawas

watershed varies with a pitch of < 8% being the most expansive area and a hill of > 45% being the smallest (see Figure 4). The headwaters include Mount Kerinci which is part of the Kerinci Seblat National Park (TNKS), designated as part of the lungs of the world, and functions as a protected forest. It is pertinent to state that the total economic value of the TNKS area is based on the direct use and residual water values. The indirect use value is associated with carbon sequestration as well as its existence (existence) and inheritance (legacy).

4.2.1. Soil Texture

Rawas watershed has unconsolidated sediments ranging from clay to sand sequences of different grades. It geologically includes highlands and lowlands and also serves as a quarter alluvial deposit from the Pleistocene to young age. Some parts of the basin have loamy sand formations due to silt deposits which are sometimes interspersed with sand. Moreover, shallow aquifers occur mainly in river deposits and meandering rivers.

4.2.2. Geomorphology

The Rawas River basin was founded on quarterly alluvial deposits consisting of clay, silt, sand, and gravel of different grades. The two groundwater samples in the field were deemed unfit for drinking based on their total dissolved solids content but all the samples were found useful for irrigation.

4.3 Land Use

Land use dramatically determines the magnitude of the soil loss index (F) and overland flow (Q). Moreover, there are different types of land use due to the influence of various coefficients of run-off (c) and the percentage of rainfall entering the soil (A). The land use map was used to generate the area and run-off coefficient values.

The map shows that the dense forest has the largest land use area in the watershed with 247120.77 Ha while residential areas have the least with 70.57 Ha (see Fig. 4).

4.4. Hydrology

A hydrological analysis was used to understand the nature of the aquifer. This is necessary because the availability of groundwater in the alluvial zone is controlled by the thickness of the sand and clay zone. The groundwater near the surface is usually under free aquifer conditions while deeper waters are due to the z (depth) limited to confined aquifer conditions. It is important to note that rainfall is the primary source to replenish groundwater in the basin and the water level shows a deteriorating trend in some parts of the study area due to rapid urbanization and intensive pumping. Moreover, the average hydraulic gradient was found to be 0.35 m/km and this means the formation near the surface of the watershed is porous.

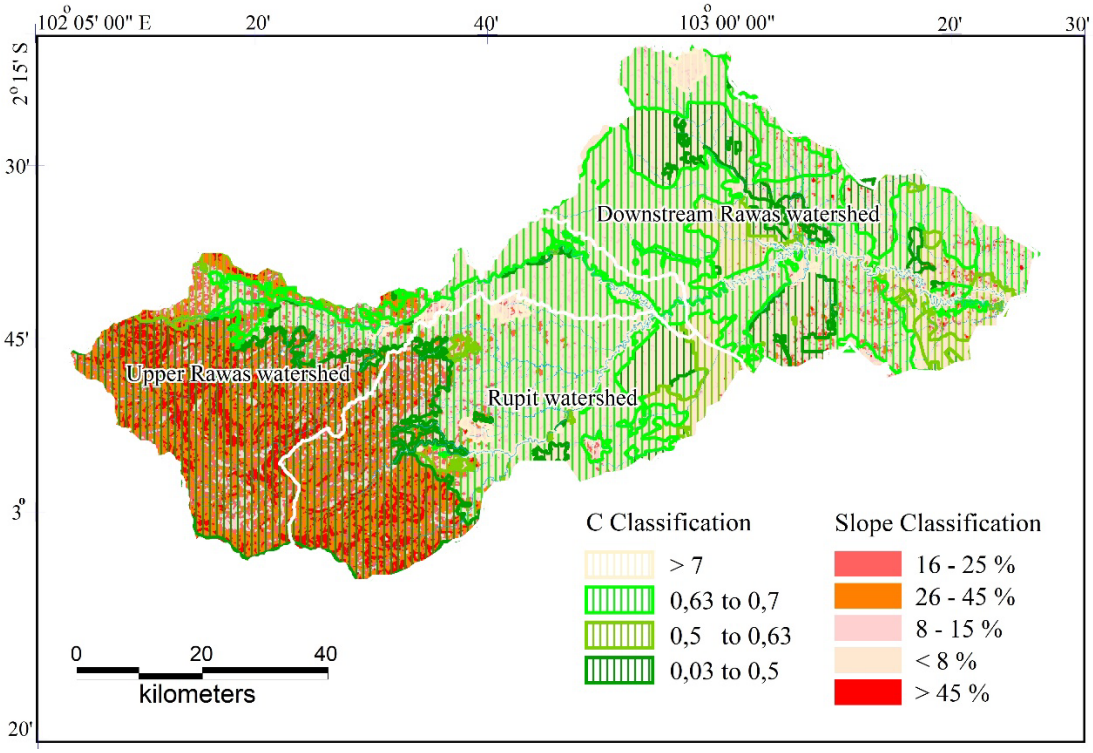

Fig. 4 Slope and C value classification

The water yield of the Rawas watershed in the form of river flow is strongly influenced by the rain input and the physical parameters of the watershed. It is important to note that the characteristics of each watershed usually lead to different water production at the same amount of rain input and vice versa. The daily rainfall in the Rawas watershed was mostly classified as 24.00 - < 46 mm/day with the highest being 78.18 - < 121 mm/day and the lowest being 0 - < 18.91 mm/day.

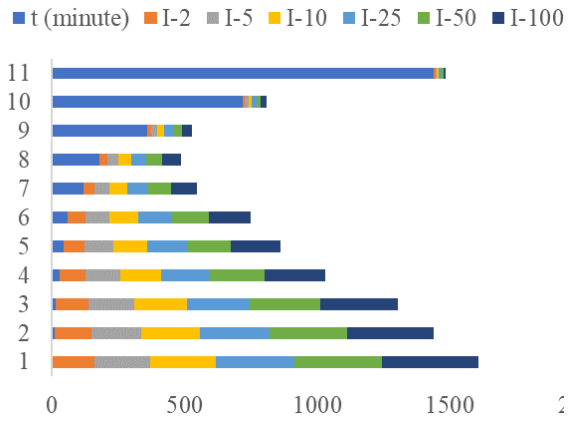

Fig. 5 IDF graph (Talbot's method), design rain intensity I_{30} (minutes) for return period 2-100 years (Srikaton Station). Line graph number three is a count of rain intensity for 30 minutes (I_{30})

4.5 Soil Erotion Estimation

Critical land is one of the indicators of ecological and environmental damage. This is due to the fact that damaged land automatically has a reduced function and role. The amount of run-off and soil erosion analyzed for a period of ten years (2010-2020) showed Fig.6, that the critical land in the Rawas watershed covers an area of 221,530,294 Ha in the crucial category, 1,078,033 Ha in the introductory, 62,930, 110 Ha in the moderate, 225,692,387 in potential critical and only 72,587,452 Ha (6.31%) was found not to be critical (see Table 3). Moreover, the problem observed to be most prominent in the watershed is the damage to natural resources such as soil, water, and vegetation due to soil erosion, landslides, degradation of soil fertility, floods, and droughts.

The general problems associated with the watershed environment were grouped into 4 (four) parts according to their respective specifications as follows:

(1) Physiographic problems associated with the relief/mountainous and hilly topography as well as the steep slopes in the upstream area including the Kerinci Seblat National Park/Mount Kerinci. It was discovered that there is a lot of illegal forest clearing by residents in search of gold ore and this led to high erosions because the land in the hill area tends to be open. Moreover, the high rainfall in the area is causing an increase in surface run-off, low soil stability, an increase in surface erosion, reduced soil fertility, and a subsequent rapid decline in soil productivity.

(2) Problems with the use of natural resources such as the destruction or burning of forests, shifting cultivation, grazing, illegal mining of uncontrolled gold ore, land clearing and conversion for oil palm plantations, and others are reducing the availability of water in the watershed area.

(3) Problems with the final process or mechanisms such as erosion–high sedimentation, floods and droughts, water pollution, eutrophication, and others.

(4) Socio-economic and population problems in the form of illiteracy, underdevelopment, poverty, lack of trained or skilled workers, status or property rights to land, lack of facilities and infrastructure, and others that are leading to poor land management.

These four problems were observed to be interrelated. This is because the socioeconomic and development pressures are leading to an increase in population can eventually intensify the biophysical damage to the watershed (watershed criticality). A new problem also arose from these conditions in the form of spatial planning or land use and observed to be very common in Indonesia due to the usage of land without considering its ability.

Table 3 Distribution and area of critical land in the sub-watershed

Watershed	Not Critical	Critical Enough	Critical Potential	Critical	Very Critical
			Ha		
Upstream Rawas	32.425,75	8.978,37	92.323,00	42.300,16	149,12
Downstream Rawas	10.167,39	38.065,97	35.219,01	142.394,57	444,25
Rupit	29.965,82	15.846,26	98.022,09	36.756,51	484,67

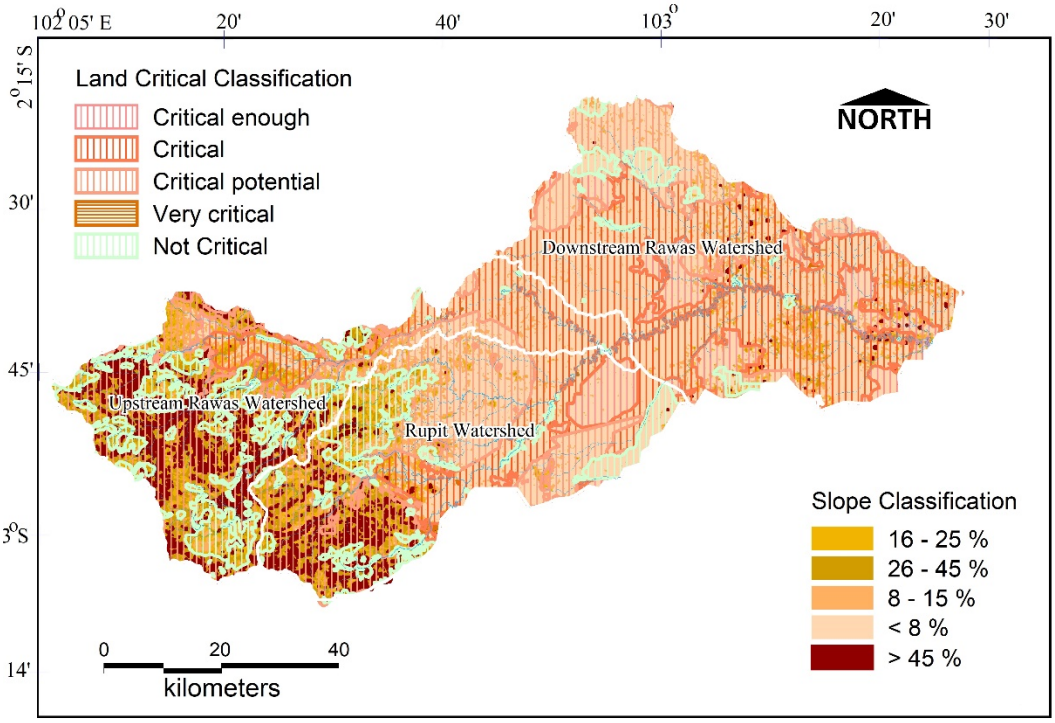

Fig. 6 Slope classification and criticality level of rawas watershed due to land use change

5. CONCLUSIONS

The main characteristics of critical land are bare, arid, and even the appearance of rocks on the ground surface. The topography is also generally hilly or steeply sloped [23] and characterized by reeds vegetation with a relatively low soil pH estimated at 4.8-6.2. The largest area of critical land in the Rawas watershed was found to be dominated by Rawas Ulu and Muara Rupit sub-districts. It was further discovered that plantation and production forest space cover 8% - 25% slope and the area classified as critical, moderately critical, and potentially critical were also found in Rupit District on a hill of 8% - 25%.

Moreover, the land allocation in the area is for food crop agriculture, production forests, and plantations in line with the direction of the South Sumatra Province Spatial Plan (RTRWP). The dominance of critical land in areas with slopes of 8% - 25% and >45% indicates that the erosion caused by high rainfall in the upstream region and inappropriate land management is the leading cause of the critical lands found in the Rawas watershed.

6. ACKNOWLEDGMENTS

The authors are grateful to the Directorate of Research Technology and Community Service, Directorate General of Higher Education, Research and Technology, Ministry of Education, Culture, Research and Technology, the Republic of Indonesia, for providing research funds through Doctoral Research Grant No. SPPK: 142/E5/PG.02.00.PT/2022, Universitas Sriwijaya, DIPA Date: November 17, 2021 with No. DIPA: SP DIPA-023.17.1.690523/2022. The authors also acknowledge the efforts of the Doctoral Programs in Engineering, Faculty of Engineering, Universitas Sriwijaya for providing the opportunity to study the activities in the Rawas sub-watershed area.

7. REFERENCES

[1] Comeliu O.D, Gottfried S.B, Anna P.S, Bartoz.K, Understanding satellite images: a data mining module for Sentinel images, Big Earth Data, vol. 05, no. 02, 2020, pp. 1–42.

[2] Gregory Giuliani, B. Chatenoux, A. Benvenuti, Lacroix, Matia.S, and Paolo Mazzetti, Monitoring land degradation at national level using satellite Earth Observation time-series data to support SDG15 – exploring the potential of data cube., Big Earth Data, vol. 4, no. 1,2020, pp. 3–22.

[3] Jing Wang, W. Zhao, G. Wang, Sigi Yang, and Paulo Pereira, Effects of long-term afforestation and natural grassland recovery on soil properties and quality in Loess Plateau (China), Sci. Total Environ., vol. 770, 2021, pp 144-158.

[4] Mengie, M.A, Y.G. Hagos, D. A. Malede, and

T. G. Andualem, Assessment of soil loss rate using GIS–RUSLE interface in Tashat Watershed, Northwestern Ethiopia, Journal. Sediment. Environment., vol. 7, no. 3,2022, pp. 617–631.

[5] Ilan Chabay, Land degradation and restoration, Companion To Environmental Studies, 1st Edition, 2018. pp. 6-20

[6] Mariano G.R, Z.Voleff, Synergizing global tools to monitor progress towards land degradation neutrality: Trends.Earth and the World Overview of Conservation Approaches and Technologies sustainable land management database, Environmental. Science Policy, vol. 93, issue November 2018, 2019. pp. 34–42.

[7] Andi Patriadi, Ria Asih, Aryani Sumitro, Dwa D.W, Wasis Wardoyo, Thosifumi Makunoki and Gozo Fujimoto., The Influence of Sembayat Weir on Sediment Transport Rate in the Estuary of Bengawan Solo River, Indonesia, Int. J. GEOMATE, vol. 20, no. 81, 2021, pp. 35–43.

[8] Paringit, M.C.R., M.D.L. Cutora, E.H. Santiago, and M.A.Q. Adajar, Assessment of landslide susceptibility: A case study of Carabao mountain in Baguio city, Int. J. GEOMATE, vol. 19, no. 71, 2020, pp. 166–173.

[9] Moonrut, N., Takrattanasaran, T.Khamkajorn and P.Chaikaew, Integrated remote sensing and GIS approaches for land degradation neutrality (LDN) assessment in the agricultural area, IOP Conf. Series: Earth and Environmental Science 626, 2021, pp. 1-7

[10] Diana Hapsari, Takeo Ohnishi and Masateru Senge, Sediment characteristics of two coniferous and broadleaf forests in Kuraiyama, Japan, Int. J. GEOMATE, vol. 20, no. 82,2021, pp. 77–85.

[11] Tjaturahono, B.S, Wahid Akhsin B.N.S, and Satya B.N, Land Cover Change Analysis To Sedimentation Rate of Rawapening Lake, Int. J. GEOMATE, vol. 18, no. 70, 2020. pp. 294–301.

[12] Sarino, Yuono A.L., and D.D.A Putranto, Spatial pattern of sediment transport for analysis of precipitation direction and magnitude in the upper Lematang river sub-basin, IOP Conf. Ser. Earth Environmental. Science., vol. 389, no. 1, 2019, pp. 1-8.

[13] Sims, N.C., Newnham, G.J., England, J.R., Guerschman, J., Cox, S.J.D., Roxburgh, S.H., Viscarra Rossel, R.A., Fritz, S. and Wheeler, Good Practice Guidance for Sustainable Development Goal (SDG) indicator 15.3.1., Proportion of Land that is degraded over total land area, Version 2.0. United Nations Convention to Combat Desertification, Bonn, Germany, Vol. 1., 2021.pp. 7-81.

[14] Dinar D.A.P, Sarino, Yuono, A.L, J.C. Imroatul, and S.A. Hamim, Integration of surface water management in urban and regional spatial planning, Int. J. GEOMATE, vol. 14, no. 45, 2018.pp 28-34.

[15] Yuono, A.L., Dinar D.A.P, and Sarino, Effect of land use changes of upstream komering sub watershed on declining water availability," J. Ecol. Eng., vol. 21, no. 2, 2020, pp. 126-130.

[16] María F.R, Julián Campo, Jesús R.C and Saskia D. Keesstra, Comparative analysis of splash erosion devices for rainfall simulation experiments: A laboratory study, Water (Switzerland), vol. 11, issue. 6, 2019.pp. 1-21.

[17] Nega T. Endalamaw, M.A. Moges, Y.S. Kebede, B.M. Alehegn, and B.G. Sinshaw, "Potential soil loss estimation for conservation planning, upper Blue Nile Basin, Ethiopia," Environ. Challenges, vol. 5, 2021, pp. 1784-1795

[18] Tayebzadeh Moghadam, K.C. Abbaspour, B. Malekmohammadi, M. Schirmer, and A. R. Yavari, Spatiotemporal Modelling of Water Balance Components in Response to Climate and Landuse Changes in a Heterogeneous Mountainous Catchment, Water Resource. Management., vol. 35, no. 3, 2021, pp. 793–810.

[19] Maria Michalopoulou, Nikolaos Depountis, Konstantinos Nikolakopoulos and Vasileios Boumpoulis, The Significance of Digital Elevation Models in the Calculation of LS Factor and Soil Erosion, Land, MDPI, 11, 1592, 2022, pp. 1-36.

[20] Siyuan Feng, Wenwu Zhao, Tianyu Zhan, Y.Y Pereira, Paulo Pereira, Land degradation neutrality: A review of progress and perspectives, Ecological Indicator., vol. 144, September, 2022, pp. 109-125.

[21] Panditharathne, D. Abeysingha, N, Nirmanee K, Mallawatantri, A, Application of Revised Universal Soil Loss Equation (RUSLE) Model to Assess Soil Erosion in Kalu Ganga River Basin in Sri Lanka, Applied and Environmental Soil Science, vol.16, 2019, pp. 209-215.

[22] Zarafshar. M, Bazot. S, Matinizadeh. M, Bordbar. S, Rousta. M, Kooch. Y, Enayati. K, Abbasi. A, Negahdarsaber. M, Do tree plantations or cultivated fields have the same ability to maintain soil quality as natural forests., Appl. Soil Ecol., vol. 151, July, 2020. pp. 103-115.

[23] Husnain Tansar, Huang F.D, and Ole Mark, Catchment-Scale and Local-Scale Based Evaluation of LID Effectiveness on Urban Drainage System Performance, Water Resources Management., vol. 36, no. 2, 2022,

pp. 507–526.
[24] Bharath, K., Kumar, K, R. Maddamsetty, M. Manjunatha, R. B. Tangadagi, and S. Preethi, Drainage morphometry based sub-watershed prioritization of Kalinadi basin using geospatial technology, Environ. Challenges, vol. 5, Issue : June, 2021, pp. 102-117.
[25] Munoth, P., and R. Goyal, Hydromorphological analysis of Upper Tapi River Sub-basin, India, using QSWAT model, Model. Earth Syst. Environ., vol. 6, no. 4, 2020, pp. 2111–2127.
[26] Agus Suharyanto, E. Suhartanto, and S. B. Lesmana, Watershed morphometric classification analysis using geographic information system, Int. J. GEOMATE, vol. 19, no. 74, 2020, pp. 114–122.
[27] Ammar Ak Ali, Alla M. Al-abbadi, Fadhil K. Jabbar, Hassan Alzahrani, and Samie Hamad, Predicting Soil Erosion Rate at Transboundary Sub-Watersheds in Ali Gharbi, Southern Iraq using RUSLE based GIS-Model, Suistanibility, MDPI, Vo. 15. 1776, 2023, pp. 1–16.
[28] Yaswanth Kaimudin, M. Kona, S. K. Andra, and M. Rathinasamy, Understanding the impact of changes in land-use land-cover and rainfall patterns on soil erosion rates using the RUSLE model and GIS techniques: A study on the Nagavali River basin, Journal Water Climate Change., vol. 13, no. 7, 2022, pp. 2648–2670.
[29] Simon Scheper, S. Tresch, and K. Meusburger, Methods X Corrigendum to ‘ Modification of the RUSLE slope length and steepness factor (LS-factor) based on rainfall experiments at steep alpine grasslands, Journal Methods X, vol. 8, 2021, pp. 2019-2029.
[30] Chaolei Zheng and Li Jia, Global canopy rainfall interception loss derived from satellite earth observations, Ecohydrology, vol. 13, no. 2, 2020, pp. 1–13.
[31] Andrew A.U, J.O. Ajiboye, E.S. Ibrahim, E. N. Gajere, A. Itse, and H. A. Shaba, Soil Loss Estimation Using Remote Sensing and RUSLE Model in Koromi-Federe Catchment Area of Jos-East LGA, Plateau State, Nigeria, Geomatics, vol. 2, no. 4, 2022, pp. 499–517.